

Catalysis Science & Technology

Accepted Manuscript



This is an *Accepted Manuscript*, which has been through the Royal Society of Chemistry peer review process and has been accepted for publication.

Accepted Manuscripts are published online shortly after acceptance, before technical editing, formatting and proof reading. Using this free service, authors can make their results available to the community, in citable form, before we publish the edited article. We will replace this *Accepted Manuscript* with the edited and formatted *Advance Article* as soon as it is available.

You can find more information about *Accepted Manuscripts* in the [Information for Authors](#).

Please note that technical editing may introduce minor changes to the text and/or graphics, which may alter content. The journal's standard [Terms & Conditions](#) and the [Ethical guidelines](#) still apply. In no event shall the Royal Society of Chemistry be held responsible for any errors or omissions in this *Accepted Manuscript* or any consequences arising from the use of any information it contains.

Investigation of the active species in the carbon-supported gold catalyst for acetylene hydrochlorination

Xi Liu,¹ Marco Conte,¹ David Elias,¹ Li Lu,² David J. Morgan,¹ Simon J. Freakley,¹ Peter Johnston,³ Christopher J. Kiely² and Graham J. Hutchings^{1*}

¹Cardiff Catalysis Institute, School of Chemistry, Cardiff University, Cardiff, CF10 3AT

²Department of Materials Science and Engineering, Lehigh University, 5 East Packer Avenue, Bethlehem, PA 18015, USA.

³Process Technologies, Johnson Matthey plc, Orchard Road, Royston, SG8 5HE

Abstract

The nature of the active species in carbon-supported gold catalysts used for synthesis of vinyl chloride monomer from acetylene hydrochlorination has been investigated using X-ray photoelectron spectroscopy and electron microscopy. Catalysts prepared by impregnation of chloroauric acid dissolved in *aqua regia* are initially inactive. During the initial reaction they show a pronounced induction period and we have used this opportunity to examine the evolution of the active catalyst as it is transformed during acetylene hydrochlorination. The fresh catalyst comprises a Au(III) surface film which on reaction with acetylene and HCl transforms to a mixture of Au(I) /Au(III). Experiments in which the catalyst is exposed sequentially to HCl and acetylene show that high activity is associated with a catalyst containing significant amounts of cations with both oxidation states and that the Au(I) and Au(III) oxidation cycle is important in the activation of both molecules. These findings are discussed in relation to the nature of the active species.

Introduction

Vinyl chloride monomer (VCM) is a major commodity chemical used in the manufacture of over 30 million tons of polyvinyl chloride (PVC) annually world-wide.^{1,2} There are two major production routes for the synthesis of vinyl chloride; namely the oxychlorination of ethane which is an oil-based process, and the hydrochlorination of acetylene which is a coal-based process.^{1,2} In recent years the hydrochlorination route has become dominant and in China over 20 million tons of vinyl chloride are manufactured annually via this method using a carbon-supported mercuric chloride catalyst in a fixed bed flow reactor.³ This catalyst is unstable and at the reaction temperature of 180 °C the mercuric chloride is gradually lost from the catalyst (typically 0.6 kg/ton VCM) and eventually this finds its way into the environment.³ This environmental pollution problem has led the Chinese Government to call for the development of a stable non-mercury based catalyst for acetylene hydrochlorination.⁴ Indeed, over 50% of the mercury ore mined annually is used to produce the catalysts for the acetylene hydrochlorination reaction.

In 1985 gold was predicted to be the best catalyst for acetylene hydrochlorination⁵ and this has subsequently been confirmed to be the case.⁶ This initiated the development of many gold-catalyzed reactions.⁷ Supported gold catalysts can be very stable and do not leach metal from the catalyst, which is in complete contrast with the supported mercuric chloride catalysts.⁶ The gold catalysts were found to comprise gold nanoparticles^{8,9} and early studies suggested that Au³⁺ on the surface of these nanoparticles was associated with high activity.^{8,9} However, this hypothesis was based largely on the characterisation and comparison of fresh and used catalysts.¹⁰ Recently there has been an resurgence of interest in finding commercially viable non-mercury catalysts for this important industrial process and most of these studies have focused on the use of gold as a catalyst.¹¹⁻¹⁴ Indeed, a recent report shows that a supported gold catalyst has been successfully used in a pilot plant for several thousand

hours without loss of activity.¹⁴ This underlines the commercial interest and significant potential of supported gold as a catalyst for acetylene hydrochlorination, leading to increased interest in this field;¹⁵⁻¹⁷ indeed, we have recently shown that these gold catalysts for VCM production are being commercialised.¹⁸

A number of previous studies have suggested that the presence of Au³⁺ is important for high activity observed in acetylene hydrochlorination.⁸⁻¹⁰ In some catalysts, lanthanides are deliberately added in order to stabilise the higher valence state of gold.¹⁹⁻²¹ Evidence to support this conjecture comes from X-ray photoelectron spectroscopy (XPS) of the fresh and deactivated catalysts where the concentration of Au³⁺ is largely depleted in the deactivated catalyst.⁸⁻¹⁰ Interestingly, transmission electron microscopy studies showed that there was very little sintering of the gold nanoparticles following deactivation.¹⁰ Studies with Mössbauer spectroscopy²² and reactivation using nitric oxide²³ confirmed the importance of the presence of cationic gold for activity. Supported gold catalysts are remarkably stable for acetylene hydrochlorination, as confirmed by recent pilot plant studies.^{14,18} Indeed, gold is the most stable catalyst of all those evaluated to date.^{6,8,9} Gold catalysts prepared using *aqua regia* do, however, deactivate slowly with time and there are two degradation pathways that have been identified. At low reaction temperatures (below 100 °C) carbon deposition by polymerisation of the vinyl chloride is observed, while at higher temperatures (above 180 °C), and typically those at which the reaction readily proceeds, deactivation is considered to be associated with the reduction of the active gold species.^{8,9}

In this study we present a detailed analysis of the catalyst during the start-up phase using a combination of X-ray photoelectron spectroscopy and electron microscopy. We show that while Au³⁺ is important in the initial phase, Au⁺ has to be present for high activity to be observed. It is the combination of acetylene and HCl during the reaction that establishes the active Au³⁺ - Au⁺ couple, and it is proposed that these couples are formed and continuously

reformed during the reaction that leads to the very long catalyst lifetimes that can be achieved with supported gold catalysts for acetylene hydrochlorination.

Experimental

Catalyst preparation

The catalysts were prepared by a modified wet impregnation method. The gold precursor, $\text{HAuCl}_4 \cdot x\text{H}_2\text{O}$ (Alfa Aesar, 40 mg, assay 49%) was dissolved in an acidic solution (HCl (Fisher, 32wt%), HNO_3 (Fisher, 70wt%), or *aqua regia* (3:1 HCl (Fisher, 32%): HNO_3 (Fisher, 70%)). These solutions were added dropwise with stirring to the activated carbon support (Norit ROX 0.8) (1.98 g) in order to obtain catalysts with a final metal loading of 1 wt%. A 1 wt% Au catalyst was similarly prepared by dissolving $\text{HAuCl}_4 \cdot x\text{H}_2\text{O}$ in water. The materials were dried (16 h, 110 °C) prior to use. The catalysts generated with water, HCl, HNO_3 and *aqua regia* solutions are labelled hereafter as Au/ H_2O /C, Au-HCl/C, Au- HNO_3 /C and Au-AR/C, respectively.

Acetylene hydrochlorination

Catalyst (150 mg) was tested for acetylene hydrochlorination in a fixed-bed glass micro-reactor. SiC (2×2.5 g) was added to extend the bed length, above and below the catalyst and this was separated from the catalyst by quartz wool. Acetylene (5 mL min^{-1} , 0.5 bar), hydrogen chloride (6 mL min^{-1} , 1 bar) and N_2 (10 mL min^{-1} , 1 bar) were fed through a mixing vessel via calibrated mass flow controllers. These gases were mixed and pre-heated to 70 °C before passing them into the heated glass reactor with a total GSHV of 740 h^{-1} . A reaction temperature of 185 °C was used. Blank tests using a reactor that was devoid of catalyst material but filled only with quartz wool and SiC did not exhibit any catalytic activity, even at 250 °C. Experiments were conducted for a fixed reaction time of 400 min.

The gas phase products were analysed by on-line by using a Varian 450 gas chromatograph equipped with a flame ionisation detector (FID). Chromatographic separation and identification of the products was carried out using a Porapak N packed column (6 ft × 1/8" stainless steel).

To monitor the evolution of gold species in the catalyst as a function of the reaction time, we undertook a systematic series of experiments using identical Au-AR/C starting materials exposed to the same reaction conditions. After specific reaction time periods the reaction was quenched by flushing the catalyst bed with N₂ while cooling to room temperature. Afterwards, the used catalysts were recovered and separated from the quartz wool. We also conducted a cycling experiment with consecutive flows of either the HCl/ C₂H₂ mixture, or HCl and C₂H₂ gases alone. First, an acetylene hydrochlorination test was conducted using Au-AR/C under the standard reaction conditions described above. Once the catalyst reached steady-state, the acetylene flow was stopped, with only HCl and N₂ flowing through the reactor for further period of 1 h. Afterwards, the HCl flow was stopped, and the catalytic bed was flushed by pure N₂ to remove residual HCl, and then the acetylene flow was restarted. After exposure to the flowing C₂H₂ /N₂ mixture for 1 h the HCl flow was restarted, and the gas composition (HCl/C₂H₂/N₂) was restored to that used in the initial experiment. Once the catalytic activity of the catalyst stabilised, we repeated the previous tests again. During the whole process, the total GSHV was maintained as 740 h⁻¹ with compensation for either C₂H₂ or HCl removal with additional N₂. At appropriate times during the second cycle of these experiments the catalysts were recovered and characterized by XPS.

XPS characterisation

XPS measurements were performed using a Kratos Axis Ultra-DLD photoelectron spectrometer employing a monochromatic aluminium K_α source operating at 144 W (10 mA

x 14 kV emission). Analysis was performed in the Hybrid mode affording greater sensitivity, over a sample area of approximately $210 \mu\text{m}^2$ at pass energies of 40 eV and 160 eV for high resolution and survey scans respectively. Charge compensation was achieved using an immersion lens system and all data were subsequently calibrated to the C(1s) core-level at 284.5 eV. All binding energies are quoted with an accuracy of $\pm 0.2\text{eV}$. Due to the propensity for cationic Au species to undergo photoreduction,²⁴ the Au(4f) spectra were collected first and then again, with all other regions of interest to minimise this effect. Data analysis was achieved using CasaXPS v2.3.17 using sensitivity factors supplied by the manufacturer.

Electron microscopy characterisation

Materials for examination by transmission electron microscopy were dry dispersed onto a holey carbon TEM grid. Since the Au had been deposited onto macroscopic extruded C support pellets, these pellets were first dry ground with an agate mortar and pestle to create some electron transparent shards. These supported fragments were examined using BF- and HAADF-STEM imaging mode in an aberration corrected JEOL ARM-200CF microscope operating at 200kV. This microscope was also equipped with a Centurio silicon drift detector (SDD) system for XEDS analysis.

Results and discussion

Effect of the solvent used in catalyst preparation

Four catalysts (Au/H₂O/C, Au-HCl/C, Au-HNO₃/C and Au-AR/C) were investigated for acetylene hydrochlorination and the results are shown in Figure 1. It is clear that the catalysts behaved very differently during the initial phase of the reaction. Au/H₂O/C was inactive over the reaction period studied using our reaction conditions. This is interesting because even

though the aqueous solution of HAuCl_4 is itself acidic, it is clear that a concentrated acid is required as a solvent with this preparation method in order to ensure activity is observed under our reaction conditions; it is possible that using a longer contact time or indeed a longer reaction time that some activity would be observed with this catalyst, but it is clearly much less reactive than any of the catalysts prepared using concentrated acids as solvents. Both Au-HCl/C and Au- HNO_3 /C show an induction period, but this is much less marked for Au-HCl/C. However, both catalysts give the same stabilised activity after 350 min time-on-line. In contrast, Au-AR/C is far more active than the catalysts prepared with the individual acids and it displays a much more distinct and extended induction period under our reaction conditions. In addition, Au-AR/C appears to exhibit a deactivation profile that is more pronounced than those exhibited by the catalysts prepared using the individual concentrated acids. In all our experiments selectivity to VCM > 99.9% was observed; no by-products such as dichlorethane were detected.

It is clear that surface functionalization of the Au/C catalysts is important. Analysis of these fresh catalysts using X-ray photoelectron spectroscopy is shown in Figure. 2 (quantitative details of the relative concentrations of the Au species present are given in the supplementary data). The choice of acidic solvent chosen for impregnation has a marked influence on the nature of the Au species present on the fresh catalyst. Indeed, Au/ H_2O /C and Au-HCl/C exhibit exclusively Au^0 , whilst Au- HNO_3 /C and Au-AR/C exhibit a mixture of Au^0 , Au^+ and Au^{3+} species. The use of *aqua regia* leads to an apparent higher degree of chlorination of the carbon (Figure 2(b)). Close inspection of the C(1s) core-level spectra (Figure 2 (c)) reveals subtle differences, specifically for Au- HNO_3 /C and Au-AR/C, where there is enhancement of the carbon signal at 288.6 eV which is concomitant with an increase in the O(1s) signal at 533.3 eV (Figure 2 (d)). Furthermore the O(1s) region for all treatments reveals some residual water (*ca.* 535 eV), whilst all acid treatments reveal a shake-up structure (*ca.* 537

eV), indicating an increase in the concentration of O-C=O species.²⁵ Hence we consider that the use of the different acids for the dissolution of H₂AuCl₄ lead to different functionalization of the carbon support thereby affecting both the dispersion and the oxidation state of the gold in the initial catalyst.

Catalyst characterisation during activation: investigating the nature of the active site

As Au-AR/C was both the most active and exhibited the most pronounced induction period we selected this material for more detailed study. We took identical individual batches of this catalyst and then subjected them to a range of reaction times. Following these times the reactor was flushed with N₂ until it had cooled down to room temperature. After removal of SiC and quartz wool, this systematic set of samples taken at different points in the activation profile were then characterised by X-ray photoelectron spectroscopy and *ex situ* aberration-corrected STEM.

Ex situ XPS of the fresh sample (Figure 3), initially shows significant concentrations of Au⁰, Au⁺ and Au³⁺ species (quantitative details of the relative concentrations are given in the supplementary data), whilst the Cl(2p) region reveals two distinct chlorine species, *ca.* 200 eV (C-Cl) and 198 eV (Au-Cl). The high initial concentration of Au³⁺ found by XPS is in good agreement with the STEM results obtained on this sample (see Figure 4). No discrete metallic gold nanoparticles were detected in this sample, although atomically dispersed Au scattered all over the carbon support could easily be observed by high angle annular dark field (HAADF) STEM imaging (Figure 4(a)). In addition occasional 2-4 nm particles containing both Au and Cl (as determined by XEDS) could also be found on the support (see Figure 4(b)). A further interesting feature commonly displayed by this sample was the presence of patches of an unstable Au containing thin film (Figure 4(c)) which under electron beam irradiation decomposed to form discrete metallic Au nanoparticles (Figure 4(d)).

Unfortunately, further discrimination of Au^{3+} and Au^+ species present *via* XPS is difficult, because the Au-Cl binding energy is identical for AuCl_3 and AuCl .²⁵⁻²⁷ Furthermore reliable $\text{Au}^{x+}:\text{Cl}$ ratios are difficult to ascertain with such cationic Au species because they are known to be highly susceptible to X-ray induced reduction.²⁴ However these experimental limitations do not nullify or compromise any qualitative deductions we have made concerning chemical state information.

HAADF-STEM images of the *aqua regia* treated Au/C sample after 30 min reaction time still showed the presence of an atomic dispersion of Au over the C support surface (Figure 5(a)), but once again discrete Au particles were completely absent. In addition, the presence of beam sensitive Au^{3+} or Au^+ containing thin films was much less obvious. Occasional particles containing both Au and Cl were detected. The example shown in Figure 5(b) is consistent with viewing tetragonal AuCl along an [001] projection in which 0.24nm (220) and (2-20) lattice fringes intersect at 90°. A second example shown in Figure 5(c) shows a tetragonal AuCl particle viewed along the [1-1-1] direction. Representative images of the *aqua regia* treated Au/C sample after 60 min are shown in Figure 6. Once again a characteristic atomic dispersion of Au was noted decorating the C surface (Figure 6(a)). Few Au containing thin films or AuCl particles were detected in this sample. Instead small (~2 nm) discrete Au particles (Figure 6(b)) and larger agglomerates of sintered Au particles (Figures 6(c),(d), (e) and (f)) were apparent. Interestingly, these latter particles were quite rounded and showed some hint of unidentified atomic scale ‘debris’ decorating their surfaces. We postulate that this could be adsorbed chloride species.

Photoelectron spectra obtained from this same systematic set of Au-AR/C samples with increasing reaction times are all rather similar to each other, albeit with small differences in the relative Au^{3+} and Au^+ concentrations (Figure 3). However, they do all show some stark differences to the fresh material. In particular, the Au^+ concentration increases markedly with

an associated decrease in the apparent Au^{3+} concentration. , Concomitant with this, there is a small upward shift of 0.4 eV in the binding energy for the Au^0 state, which could potentially be attributable to either an increase in mean Au particle size or the formation of a chlorine containing film on the surface of any Au particles.

Based on these XPS and STEM results it is clear that the catalyst evolves during the reaction upon interaction with acetylene and hydrogen chloride at the reaction temperature. The first observation is that all the samples contain individual gold atoms. The fresh catalyst also seems to comprise a surface film containing Au^{3+} yet this material is initially inactive. This suggests that the presence of Au^{3+} alone is not a sufficient condition to observe high activity. This finding is in direct contradiction to a number of our previous studies which were based solely on the examination of fresh and deactivated catalysts.^{8,9} In our previous studies we only emphasized the role of Au^{3+} in the origin of the catalyst activity. We find from XPS that as the catalyst activity increases, so does the relative proportion of Au^+ in the catalyst and this either suggests that it is the presence of an Au^+ - Au^{3+} redox couple that is important in facilitating the very selective addition of HCl to acetylene or that Au^+ is more active catalyst in this reaction than Au^{3+} .²⁸ The observation of the importance of Au^+ in the present study is in agreement with the earlier findings by Zhou *et al.*¹² Furthermore, also in homogeneous gold catalysis with alkynes the most active catalysts known are gold(I) catalysts^{7,29} and also for heterogeneous gold catalysts in the conversion of alkynes the importance of gold(I) and gold(III) has been documented.³⁰ The in situ reduction of gold(III) under catalysis conditions has (later) also been detected in homogeneous gold catalysis.³¹

Effect of sequential feeding of reactants on the catalyst: comments on the nature of the active site

To examine the nature of the active site in more detail we investigated the effect of feeding either acetylene or hydrogen chloride sequentially after the catalyst had attained full activity. We have previously shown that the acetylene/hydrogen chloride ratio is crucial in attaining high activity, and that environments rich in hydrogen chloride are required since exposure of the catalyst to excess acetylene leads to deactivation.¹⁰ Again we used Au-AR/C for these experiments and the catalytic results are shown in Figure 7. Firstly we allowed the activity of the catalyst to increase during an induction period of 100 min. We then exposed the catalyst to hydrogen chloride alone diluted with nitrogen (6 mL min⁻¹ of HCl and 15 mL min⁻¹ of N₂) and no vinyl chloride monomer formation was observed. Following this, we switched off the hydrogen chloride feed and replaced this with acetylene in nitrogen (5 mL min⁻¹ of C₂H₂ and 15 mL min⁻¹ of N₂). At this stage a small amount of acetylene conversion into vinyl chloride monomer was observed. Finally, we switched the gas feed back to the combined acetylene/hydrogen chloride reaction mixture. The catalyst, as expected had been deactivated to some extent by exposure to acetylene in the absence of hydrogen chloride as has been observed previously.²⁸ We then repeated this sequence and showed that the catalyst becomes stable to this cycling of reactants as the same steady state conversion was attained following each full set of sequential experiments (Figure 7). Samples were collected for *ex-situ* XPS analysis following the establishment of the steady state conversion (sample 1, Figure 7), after exposure to hydrogen chloride (sample 2, Figure 7) and after exposure to acetylene (sample 3, Figure 7). The results are shown in Figure 8 (quantitative details of the relative concentrations of the Au species present are given in the supplementary data). It is clear that when the steady state has been achieved, both Au⁺ and Au³⁺ species are present and the presence of Au-Cl bonds confirmed by the Cl(2p) signal at *ca.* 198 eV; no observable changes are noted for the C(1s) spectra (not shown). After exposure to just hydrogen chloride the amount of Au³⁺ present increases and the Au⁺ content decreases. Finally when the catalyst

is subsequently re-exposed to acetylene then the Au^+ concentration increases at the expense of Au^{3+} concentration. We therefore conclude that the $\text{Au}^+ - \text{Au}^{3+}$ redox couple is a key feature of the active site of this catalyst.

Finally, we decided to revisit the correlation between the catalyst activity and the standard electrode potential that initially led to gold being identified as the most active catalyst for acetylene hydrochlorination. The original correlation was based on the $\text{Au}^{3+} - \text{Au}^0$ redox couple,³² but our current findings conclude this may not be the most important active redox couple in this system. Indeed, it is known that Au^0 is inactive in the acetylene hydrochlorination reaction.⁸ Hence, we have now re-plotted the original data³³ using the appropriate chloride standard electrode potentials using the data for an $\text{Au}^+ - \text{Au}^{3+}$ couple.³⁴ The re-plotted data (Figure 9) indeed confirms that a linear correlation is obtained, adding further weight to our conclusion that the $\text{Au}^+ - \text{Au}^{3+}$ active site is formed *in situ* when acetylene and hydrogen chloride are both present. As noted earlier³³ the correlation does not hold for Pt as this catalyst rapidly deactivates from coking. It should be noted that in commercial use the Hg catalyst requires a loading of 10% to achieve a performance similar to that of a gold catalyst with much less than 1% metal loading. Furthermore, the Hg catalyst deactivates due to rapid metal loss, a feature that is not observed with the gold catalyst. As we anticipate the future full commercialisation of such supported gold catalysts for acetylene hydrochlorination,¹⁴ based on the high activity of gold catalysts containing very low levels of gold prepared using gold thiosulfate complexes,³⁵ we consider that these important new findings will significantly aid the design of improved catalyst formulations based on supported gold.

Acknowledgements

We thank the World Gold Council and Johnson Matthey for financial support.

References

1. R. L. Myers, *The 100 Most Important Chemical Compounds*, Chapter 98, Greenwood Press: Westport, 2007
2. M. Conte and G. J. Hutchings, *Modern Gold Catalyzed Synthesis*, Chapter 1, Wiley: Weinheim, 2012
3. P. J. Nat, *The Catalyst Review* 2015, 28, 8.
4. United Union, Global Mercury Assessment 2013, <http://www.unep.org/PDF/PressReleases/GlobalMercuryAssessment2013.pdf>
5. G. J. Hutchings, *J. Catal.* 1985, 96, 292-295.
6. B. Nkosi, N. J. Coville and G. J. Hutchings, *Appl. Catal.* 1988, **43**, 33 - 39.
7. A. S. K. Hashmi and G. J. Hutchings, *Angew. Chem. Int. Ed.* 2013, 52, 7963-7966
8. B. Nkosi, N. J. Coville, G. J. Hutchings, M. D. Adams, J. Friedl, and F. E. Wagner, *J. Catal.* 1991, **128**, 366 - 377.
9. B. Nkosi, M. D. Adams, N. J. Coville and G. J. Hutchings, *J. Catal.* 1991, **128**, 378 - 386.
10. M. Conte, A. F. Carley, C. Heirene, D. J. Willock, P. Johnston, A. A. Herzing, C. J. Kiely and G. J. Hutchings, *J. Catal.* 2007, **250**, 231 - 239.
11. H. Zhang, B. Dai, X. Wang, W. Li, Y. Han and J. Gu, J. Zhang, *Green Chem.* 2013, **15**, 829 - 836.
12. K. Zhou, W. Wang, Z. Zhao, G. Luo, J. T. Miller, M. S. Wong and F. Wei, *ACS Catal.* 2014, **4**, 3112 - 3116.
13. J. Xu, J. Zhao, J. Xu, T. Zhang, X. Li, X. Di, J. Ni and J. Wang, J. Cen, *Ind. Eng. Chem. Res.* 2014, **53**, 14272 - 14281.
14. K. Zhou, J. Jia, C. Li, H. Xu, J. Zhou, G. Luo and F. Wei, *Green Chem.* 2015, **17**, 356 - 364.
15. Y. Pu, J. Zhang, X. Wang, H. Zhang, L. Yu, Y. Dong and Wei Li, *Catal. Sci. Tech.* 2014, **4**, 4426-4432.
16. G. Li, W. Li and J. Zhang, *Catal. Sci. Tech.*, 2016, DOI: 10.1039/C5CY01808K
17. G. Li, W. Li and J. Zhang, *Catal. Sci. Tech.*, 2015, DOI: 10.1039/C5CY01209K
18. P. Johnston, N. Carthey and G. J. Hutchings *J. Am. Chem. Soc.* 2015, **137**, 14548 - 14557.
19. Q. Fu, H. Saltsburg and M. Flytzani-Stephanopoulos, *Science* 2003, **301**, 935 - 938.
20. S. Carrettin, P. Concepcion, A. Corma, J. M. L. Nieto and V. F. Puntes, *Angew. Chem. Int. Ed.* 2004, **43**, 2538 - 2540.
21. J. Guzman and B. C. Gates, *J. Am. Chem. Soc.* 2004, **126**, 2672 - 2673.
22. J. Friedl, F. E. Wagner, B. Nkosi, M. Towert, N. J. Coville, M. D. Adams and G. J. Hutchings, *Hyperfine Interactions* 1992, **69**, 767 - 770.
23. B. Nkosi, N. J. Coville and G. J. Hutchings, *J. Chem. Soc., Chem. Commun.* 1988, **1**, 71 - 72.

24. M. Conte, C. J. Davies, D. J. Morgan, T. E. Davies, D. J. Elias, A. F. Carley, P. Johnston and G. J. Hutchings, *J. Catal.* 2013, **297**, 128 - 136.
25. Y. Y. Fong, B. R. Visser, J. R. Gascooke, B. C. C. Cowie, L. Thomsen, G. F. Metha, M. A. Buntine and H. H. Harris, *Langmuir* 2011, **27**, 8099 - 8104.
26. G. Beamson and D. Briggs, High Resolution XPS of Organic Polymers - The Scienta ESCA300 Database, (Wiley, Chichester, 1992).
27. NIST X-ray Photoelectron Spectroscopy Database, Version 4.1 (National Institute of Standards and Technology, Gaithersburg, 2012); <http://srdata.nist.gov/xps/>.
28. N.A. Carthey, P. Johnston and M.L. Smidt, *WIPO Pat.* WO 2010/055341(A3), 2010.
29. M. C. Blanco Jaimes, F. Rominger, M. M. Pereira, R. M. B. Carrilho, S. A. C. Carabineiro and A. S. K. Hashmi, *Chem. Commun.* 2014, 4937-4940
30. S. Carrettin, M. C. Blanco, A. Corma and A. S. K. Hashmi, *Adv. Synth. Catal.* 2006, **348**, 1283-1288
31. A. S. K. Hashmi, M. C. Blanco, D. Fischer and J. W. Bats, *Eur. J. Org. Chem.* 2006, 1387-1389
32. G. J. Hutchings, *Gold Bull.* 1996, **29**, 123 - 130.
33. M. Conte, A. F. Carley, G. Attard, A. A. Herzing, C. J. Kiel and, G. J. Hutchings, *J. Catal.* 2008, **257**, 190 - 198.
34. J. J. Lingane, *J. Electroanal. Chem.* 1962, **4**, 332 - 342.
35. P.T. Bishop, N.A. Carthey and P. Johnston, *WIPO Pat.* WO 2013/008004(A3), 2013.

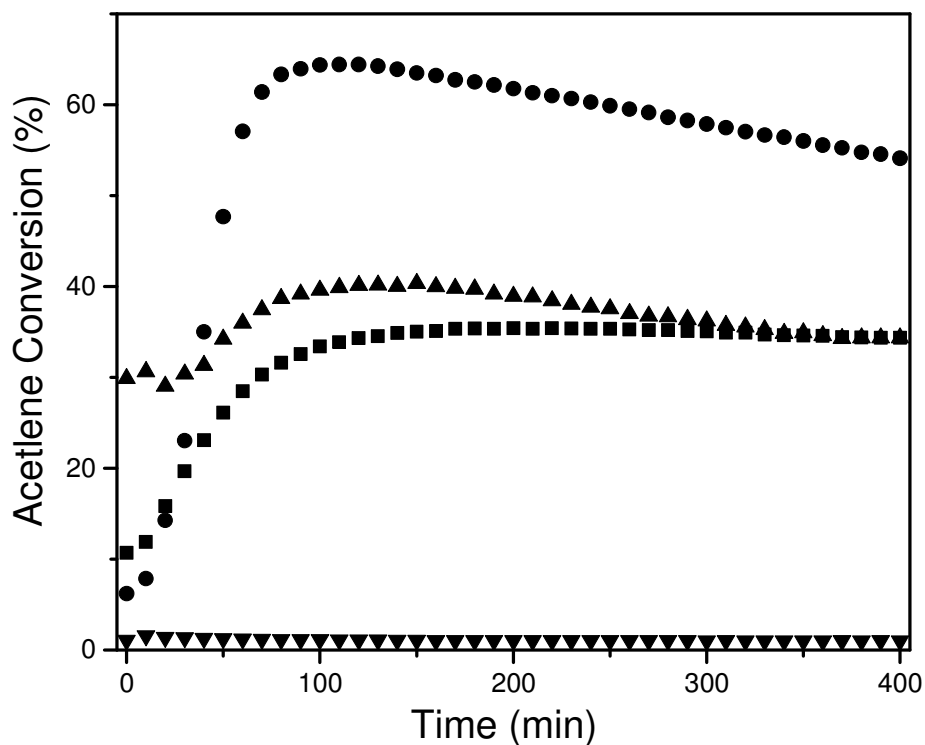


Figure 1 Catalytic performance of the supported gold catalysts as a function of reaction time, the carbon supported gold catalysts prepared from water, HCl, HNO₃ and *aqua regia*, are labelled as Au/H₂O/C (▼), Au-HCl/C (▲), Au-HNO₃/C (■) and Au-AR/C (●), respectively. All catalytic tests were conducted under identical reaction conditions: 150 mg catalyst, 5 mL/min C₂H₂, 6 mL/min HCl and 10 mL/min N₂, 185 °C.

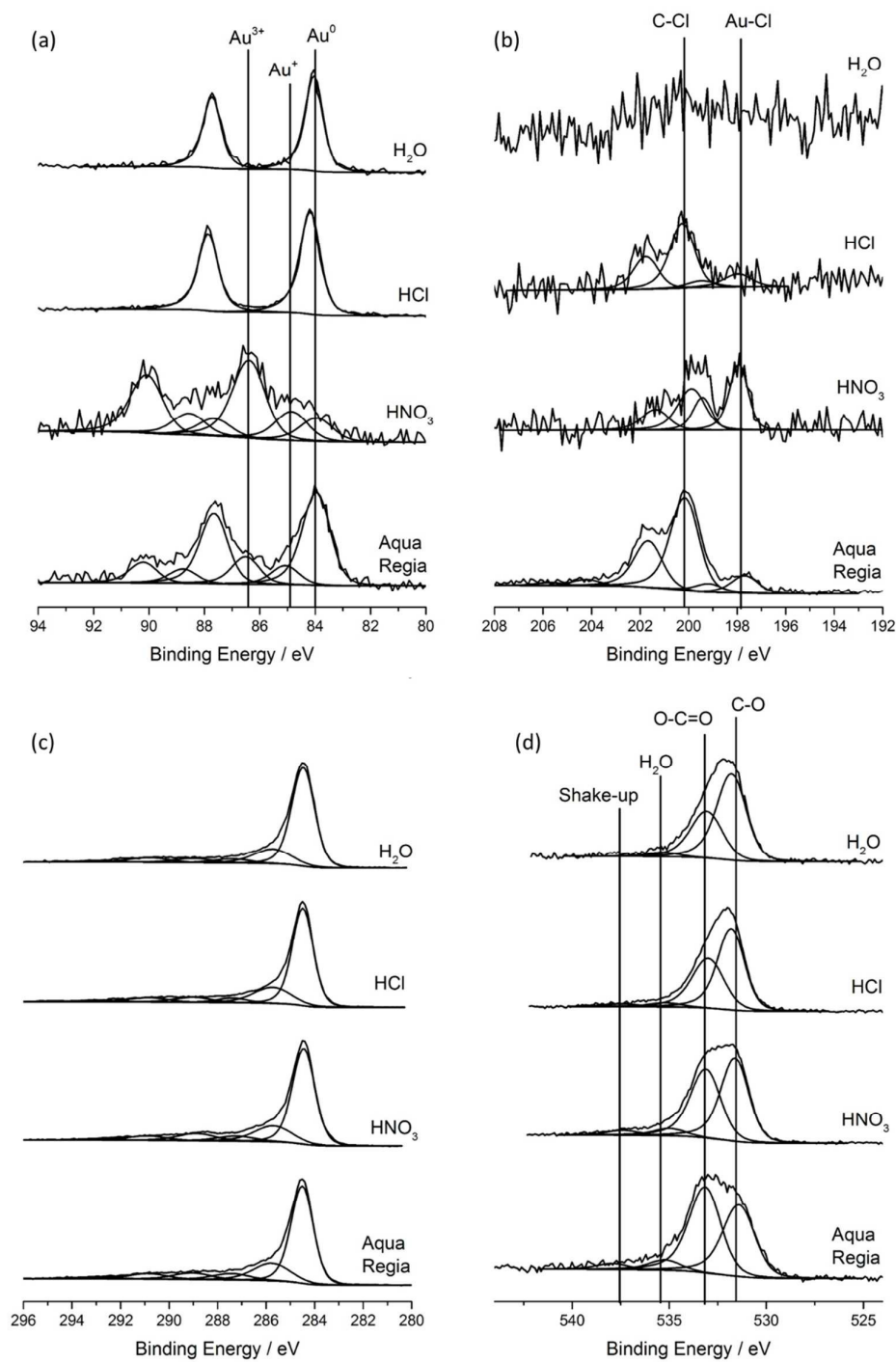


Figure 2 X-ray photoelectron core-level spectra for fresh Au/C catalysts. (a) Au(4f), (b) Cl(2p), (c) C(1s) and (d) O(1s).

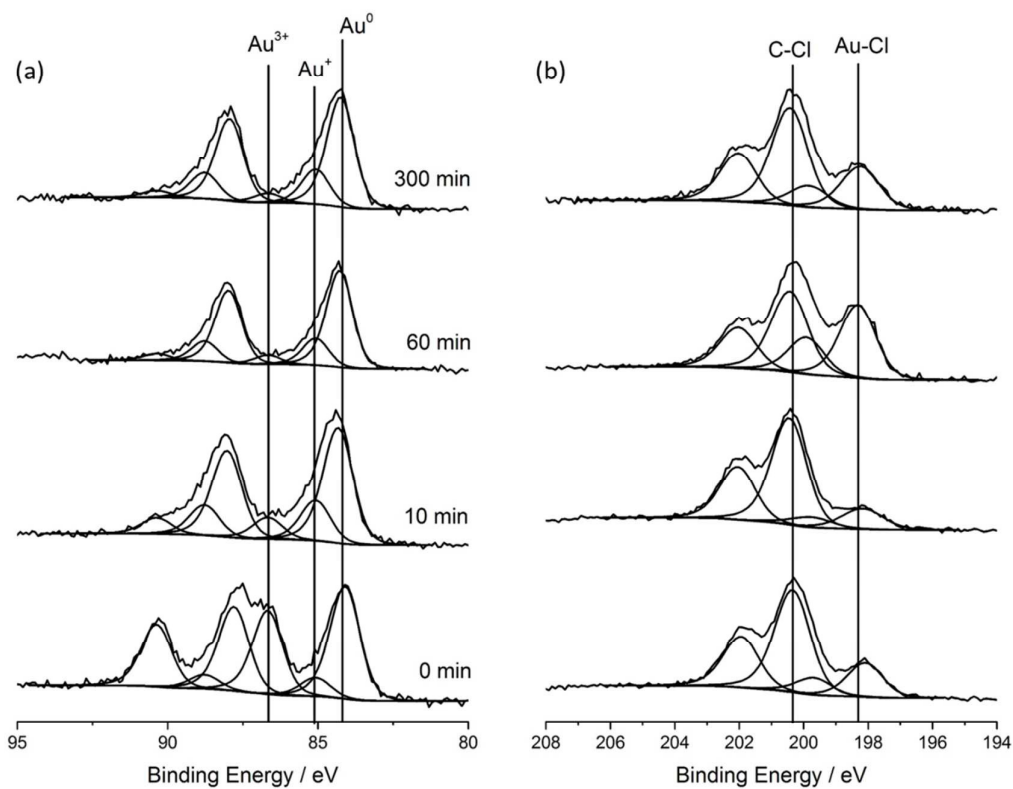


Figure 3 *ex situ* recorded X-ray photoelectron spectra for *aqua regia* prepared Au/C catalyst taken from the reactor at different times on line. (a) Au(4f) and (b) Cl(2p)

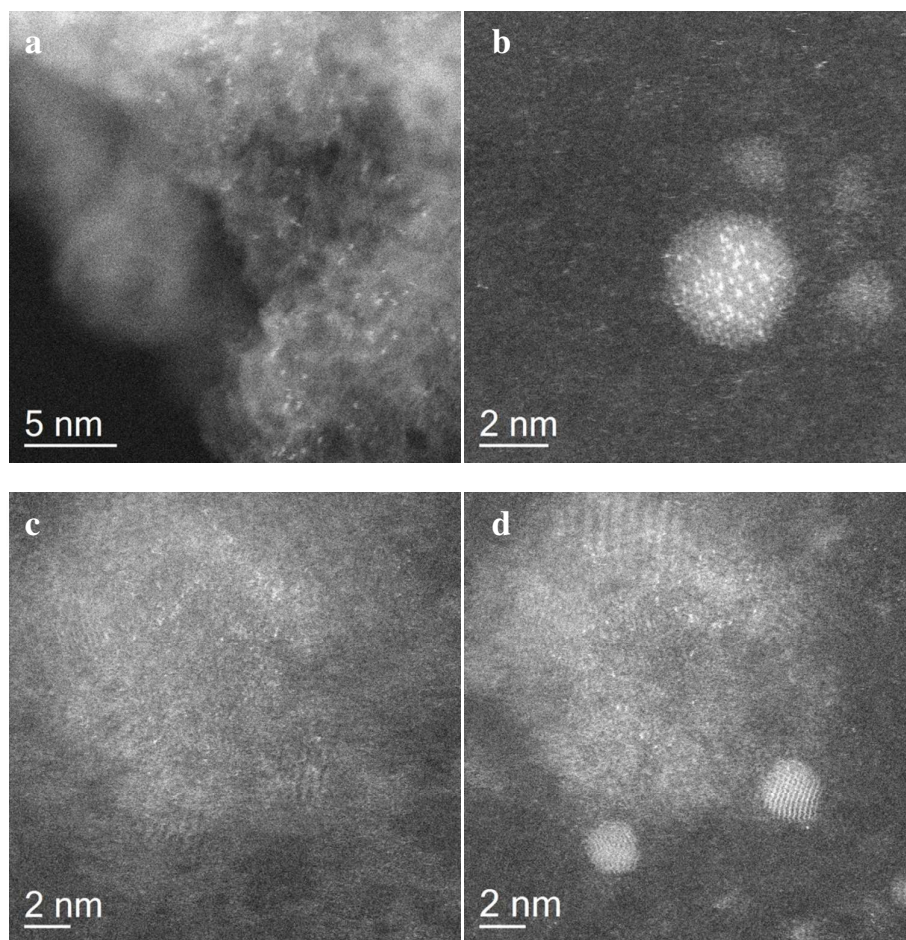


Figure 4 Representative HAADF-STEM images of the as-prepared unused *aqua regia* treated Au/C sample showing:- (a) dispersed Au atoms over the support; (b) discrete nanoparticles containing Au and Cl; and (c) unstable Au containing thin films which decompose to form Au nanoparticles (d) upon extended electron beam irradiation.

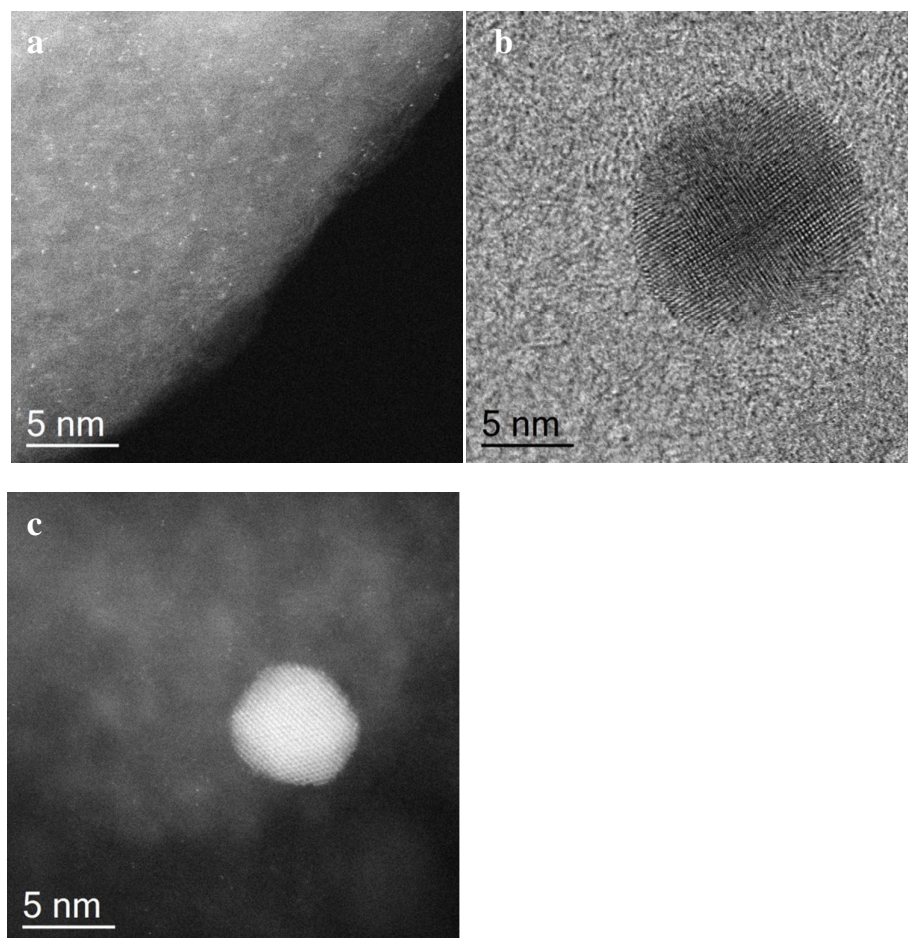


Figure 5 The *aqua regia* treated Au/C sample after 30 minutes of use:- (a) HAADF-STEM image showing discrete Au atoms decorating the support; (b) BF-STEM lattice image of a nanoparticle which is consistent with the [001] projection of tetragonal AuCl; (c) HAADF-STEM image showing some individual Au atoms and an AuCl nanoparticle viewed along the [1-1-1] projection.

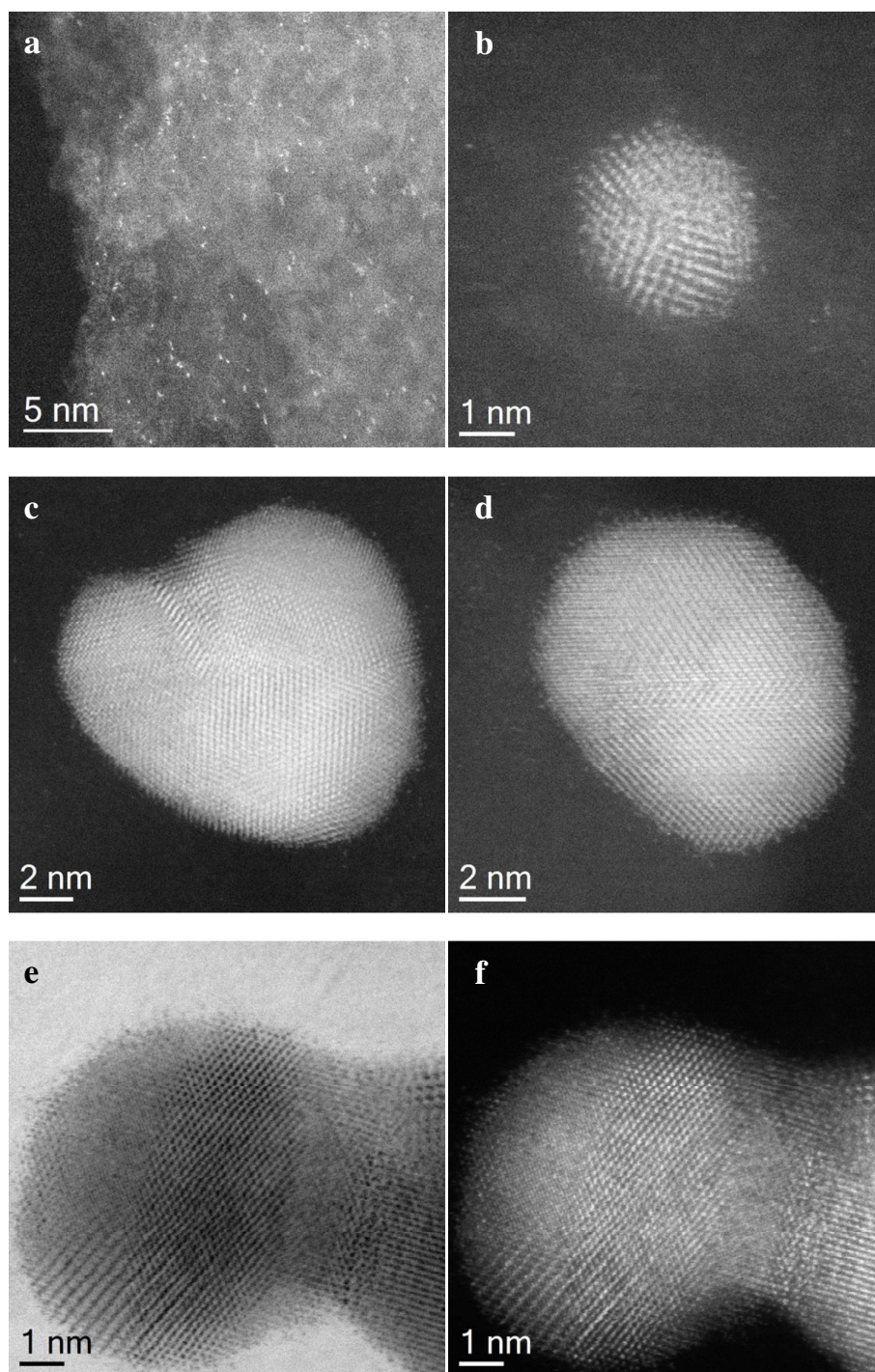


Figure 6 The *aqua regia* treated Au/C sample after 60 minutes of use:-(a) HAADF-STEM image showing discrete Au atoms decorating the support; (b) HAADF-STEM image of a discrete Au nanoparticle; (c) and (d) HAADF-STEM images of sintered agglomerates of Au nanoparticles; (e) and (f) Complimentary BF- and HAADF-STEM image pair of a sintered Au agglomerate. Note that images (c) - (f) show evidence of an unidentified debris decorating the particle surface.

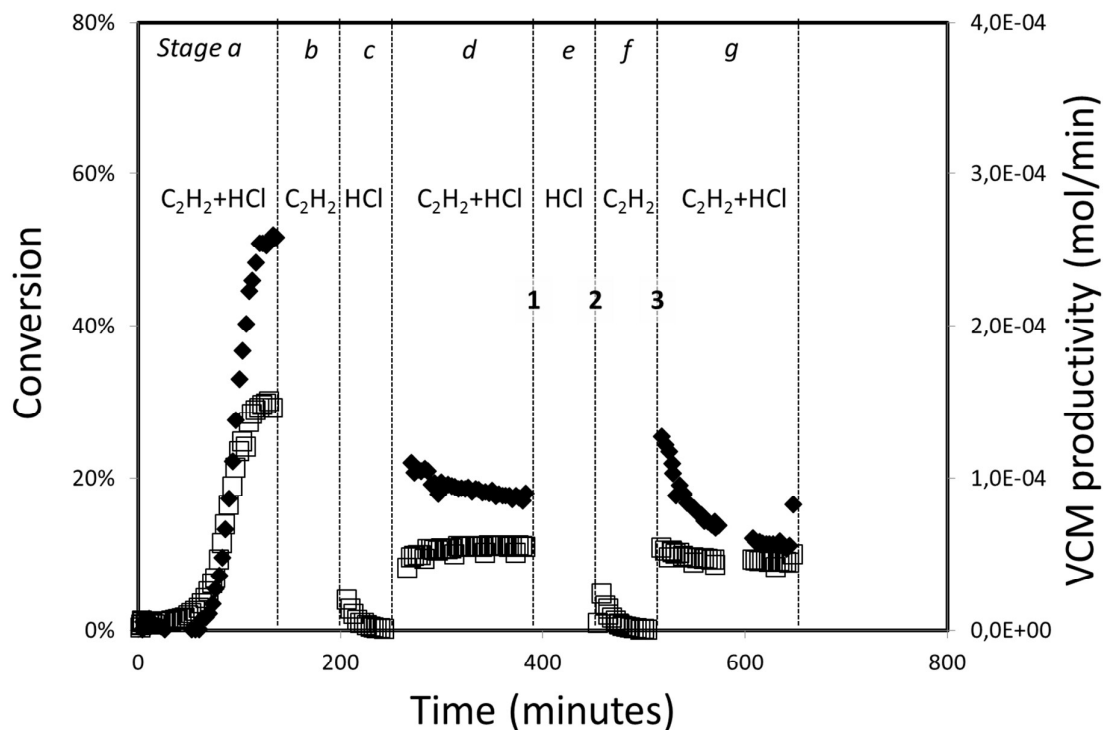


Figure 7 Cycling tests of Au-AR/C sample with consecutive flows of HCl / C₂H₂ mixture, HCl and C₂H₂ gases in sequence: Key: ◆ acetylene conversion, □ VCM productivity; firstly, (stage a) the catalyst was tested under the identical reaction condition in presence of both C₂H₂ and HCl (150 mg catalyst, 5ml/min C₂H₂, 6ml/min HCl, 10ml/min N₂, 185°C); (stage b) once the catalyst reached steady-state, C₂H₂ was switched off and the catalyst was flushed by HCl and N₂ for 1 h (6ml/min HCl, 15ml/min N₂, 185°C); afterwards, (stage c) HCl was switched off and C₂H₂ was introduced again (5ml/min C₂H₂, 16ml/min N₂, 185°C); after 1 h, (stage d) and the gas composition was restored to that used in the initial experiment (5ml/min C₂H₂, 6ml/min HCl, 10ml/min N₂, 185°C); afterwards, the same sequence was repeated again (stage e,f and g) to confirm reproducibility. The cycling tests were repeated three times, but stopped at end of stage d, e and f, respectively, the catalysts were flushed by N₂ and cooled to room temperature, after removal of SiC and quartz wool, the catalysts were characterized by XPS (Fig. 8)

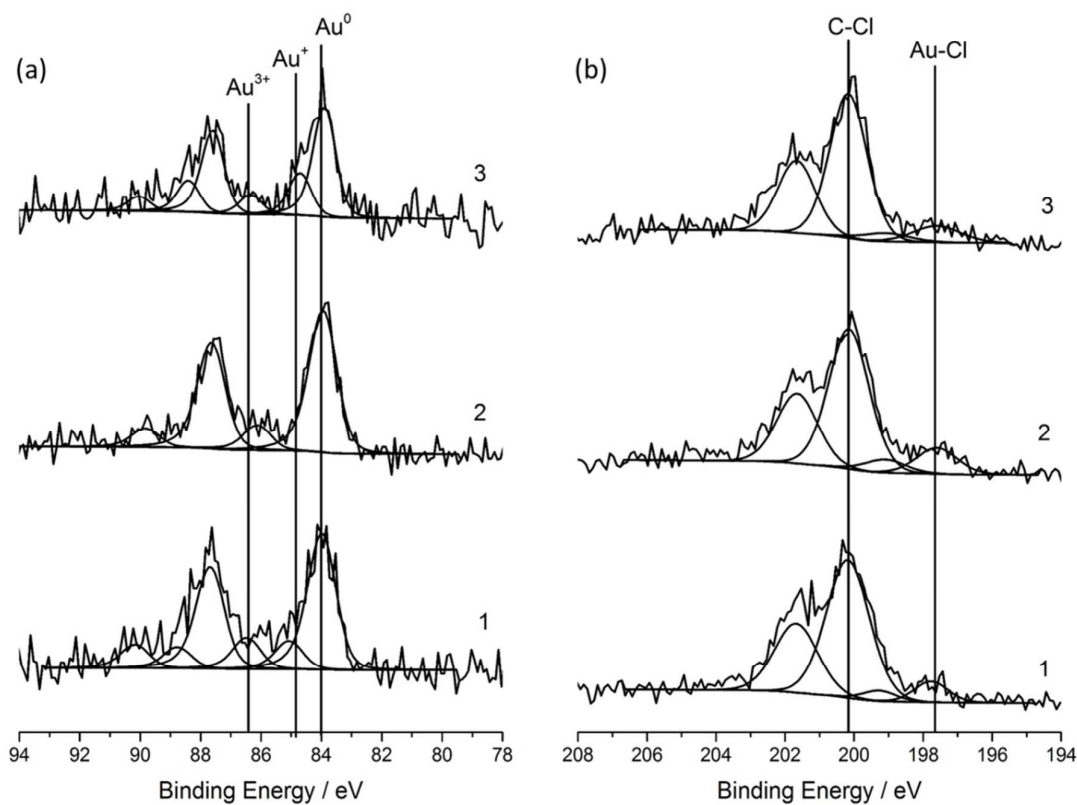


Figure 8 *ex situ* recorded core-level spectra for HCl-C₂H₂ cycling experiments (Fig. 7), where: 1 = after establishment of steady state conditions, 2 = after exposure to HCl only, and 3 = after exposure to C₂H₂ only. (a) Au(4f) and (b) Cl(2p)

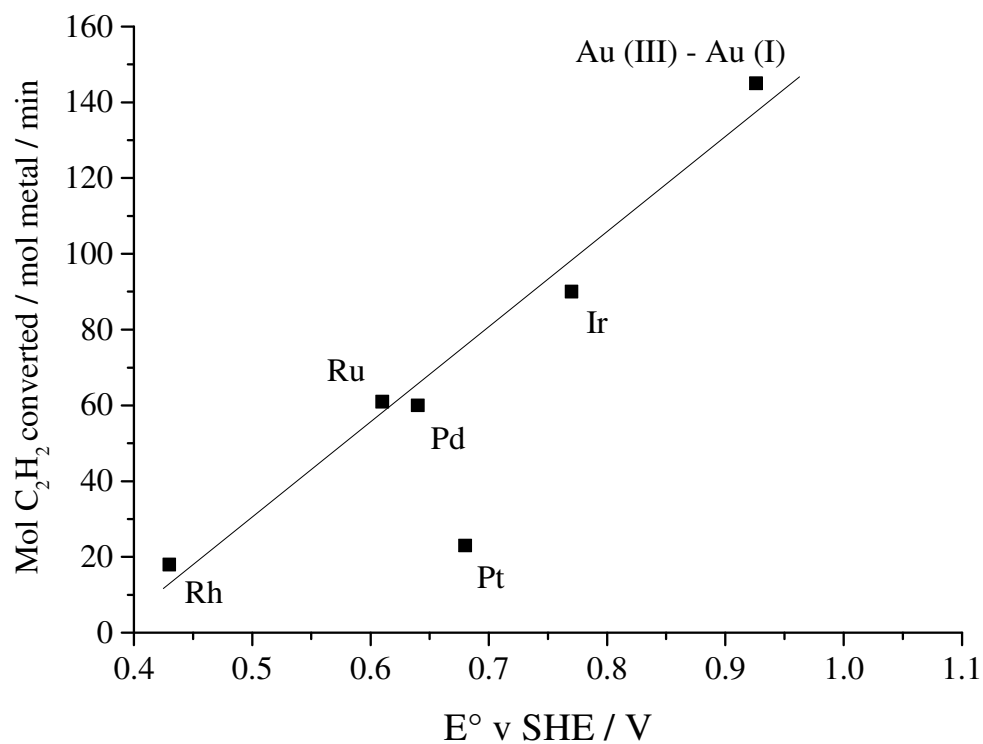


Figure 9 Correlation between activity for acetylene hydrochlorination and the standard electrode potential. Potentials are obtained from the reduction potentials of the following chloride salts (RhCl_6)³⁻, (RuCl_5)²⁻, PdCl_2 , (PtCl_6)²⁻, (IrCl_6)³⁻ (data re-plotted from reference 26; all potentials for a 2 e⁻ reduction). (AuCl_4)⁻ to (AuCl_2)⁻ potential taken from reference 27.

Graphical abstract

The active site for a Au/C catalysts for acetylene hydrochlorination involves a $\text{Au}^+ - \text{Au}^{3+}$ couple.

